Chemical Physics Letters 643 (2016) 71–76

Contents lists available at ScienceDirect

Chemical Physics Letters

journal homepage: www.elsevier.com/locate/cplett

Brute force (or not so brute) digital simulation in electrochemistry revisited

Francisco Martínez-Ortiz [a,*], Noemí Zoroa [b], Eduardo Laborda [a], Angela Molina [a]

[a] Departamento de Química Física, Facultad de Química, Regional Campus of International Excellence "Campus Mare Nostrum", Universidad de Murcia, 30100 Murcia, Spain

[b] Departamento de Estadística e Investigación Operativa, Facultad de Matemáticas, Regional Campus of International Excellence "Campus Mare Nostrum", Universidad de Murcia, 30100 Murcia, Spain

ARTICLE INFO

Article history:
Received 5 October 2015
In final form 10 November 2015
Available online 1 December 2015

ABSTRACT

The use of very high order spatial discretisation in digital simulation of electrochemical experiments is assessed, considering up to asymmetric 8-point approximations for the derivatives. A wide range of conditions are examined, including several mechanisms and electrodes and potential-step and potential-sweep experiments. In all cases it is found that asymmetric multi-point approximations in combination with exponentially expanding grids provides very accurate results and with very reduced number of grid points (<15). Consequently, the direct ('brute force') resolution of the finite-difference equation system by standard matrix techniques becomes a competitive and more general alternative to specialised methods like the Thomas algorithm.

1. Introduction

Some years ago, Britz [1] wrote a paper entitled 'Brute Force Digital Simulation in Electrochemistry'. In that work, the direct resolution of the system of equations involved in the finite difference treatment of digital simulation of electrochemical experiments was considered and related to some specialised methods such as the Thomas Algorithm in both its scalar [2,3] and matrix-vector versions [4].

More recently, some papers were published [5–8] where the direct discretisation of the mathematical laws governing the mass transport in electrochemical problems was tackled very efficiently by using multipoint higher-order approximations to the spatial derivatives. A special case was found [7] with an asymmetric four-point formula in an exponentially expanding grid which gives rise to very good results while enabling the use of very high expansion factors in the range 1.41–1.55.

In this paper, the value of other higher-order asymmetric multipoint formulae is assessed. Thus, 5-, 6-, 7- and even 8-point approximations are considered with only one point on the left-hand side of the point of the derivative (the so-called (N,2) forms). As will be demonstrated later, with these multi-point approximations very accurate results can be obtained with exceptionally high expansion factors (for example, values close to 2 can be appropriate). Thus, the (N,2) formulae show very interesting features:

(1) As above-mentioned, the (N,2) forms give rise to accurate results with very high expansions factors in the spatial grid and without numerical oscillations, in contrast with the behaviour of other multi-point formulae.
(2) The (N,2) forms are suitable for the application of Thomas-like algorithms. So, all the methodologies developed around the three-point formulae are easily extensible here.
(3) The extremely high expansion factors available under these conditions allow us to cover an extended spatial region with small interval amplitudes near the electrode surface with very, very few points in the grid. For example, a dimensionless distance of 100 (often needed for the simulation of some electrochemical techniques) with a distance of 0.1 for the point nearest to the electrode can be covered with a 12-point grid.
(4) Dealing with such very small grids, the direct resolution of the implicit systems of equations resulting from the application of finite difference methodology by standard procedures is not only possible, but convenient and very competitive in most situations.
(5) The resulting computer programs are very simple to code. In addition, the most tedious to write routines as well as some example programs are given to make it easier for occasional programmers to write their own programs fitting their demands.

* Corresponding author.
E-mail address: fmortiz@um.es (F. Martínez-Ortiz).

http://dx.doi.org/10.1016/j.cplett.2015.11.011
0009-2614/

2. Some theoretical considerations

2.1. General

The general expression for the approximation to the spatial first derivatives of the concentration of a given species, j, in a point, i, using the $(N,2)$ forms in an exponentially expanding grid is given by

$$\left(\frac{\partial c^j}{\partial x}\right)_i \approx \frac{1}{h{\gamma_e}^i}\sum_{k=i-1}^{i+N-2}\beta_{k-i}c_k^j \tag{1}$$

whereas the second derivative by

$$\left(\frac{\partial^2 c^j}{\partial x^2}\right)_i \approx \frac{1}{h^2{\gamma_e}^{2i}}\sum_{k=i-1}^{i+N-2}\alpha_{k-i}c_k^j \tag{2}$$

where i denotes the position in the grid ($i = 1, 2, \ldots$), h is the first-interval amplitude, γ_e is the expansion factor, and the coefficients α and β are given by analytical expressions independent of the position in the grid (some of them can be found in [7]). The distance, x, at point i, x_i, is

$$x_i = h\frac{{\gamma_e}^i - 1}{\gamma_e - 1} \tag{3}$$

If we consider Fick's second law, usually addressed in electrochemical problems, for a species, j, in dimensionless form,

$$\frac{\partial C^j}{\partial \tau} = \frac{\partial^2 C^j}{\partial x^2} + \frac{f}{R_0 + x}\frac{\partial C^j}{\partial x} \tag{4}$$

where f is 0, 1 or 2, for planar, cylindrical and spherical electrodes, respectively, and

$$C^j = \frac{c^j}{c^{r*}} \tag{5}$$

$$\tau = \frac{t}{t_r} \tag{6}$$

$$x = \frac{r - r_0}{\sqrt{D_j t_r}} \tag{7}$$

$$R_0 = \frac{r_0}{\sqrt{D_j t_r}} \tag{8}$$

with c^j being the concentration of species j, c^{r*} the bulk concentration of the reference species, t is time and t_r an appropriate reference time. r is the distance to the centre of the electrode (spherical and cylindrical) and r_0 is the electrode radius. For a planar electrode, x is simply the dimensionless distance from the electrode surface. D_j is the diffusion coefficient of j.

By applying (1) and (2) to the right-hand side of (4), one obtains

$$\frac{1}{h^2{\gamma_e}^{2i}}\sum_{k=i-1}^{i+N-2}\alpha_{k-i}c_k^j + \frac{f}{R_0 + x_i}\frac{1}{h{\gamma_e}^i}\sum_{k=i-1}^{i+N-2}\beta_{k-i}c_k^j \tag{9}$$

With a two-point approximation for the left-hand side term in (4), we have

$$\frac{C_i^{j'} - C_i^j}{\delta\tau} \tag{10}$$

where C_i^j represents the (known) concentration of species j at point i at the time τ, whereas $C_i^{j'}$ is the (unknown) concentration of the same species at the same point but at the time $\tau + \delta\tau$.

The combination of (9) and (10) can be given in several ways. Thus, one can take the known values C_i^j in (9) giving rise to the explicit methods (very limited and offering poor results, so, not very interesting), the unknown values $C_i^{j'}$ obtaining the fully implicit method, the average of C_i^j and $C_i^{j'}$ (the Crank-Nicolson method), a combination of smaller fully implicit time steps (the extrapolation methods) or a multipoint approximation for (10) obtaining, for example the BDF (backward differentiation formula). In any case, the most interesting question for our 'brute force' approximation is to deal with implicit methods. So, in this section the procedure will be illustrated for the case of the fully implicit (FI) method.

In the context of the FI method, the combination of (9) and (10) leads to

$$-C_i^j = -C_i^{j'} + \frac{\lambda}{{\gamma_e}^{2i}}\sum_{k=i-1}^{i+N-2}\left(\alpha_{k-i} + \frac{fh{\gamma_e}^i}{R_0 + x_i}\beta_{k-i}\right)C_k^{j'} \tag{11}$$

with

$$\lambda = \frac{\delta\tau}{h^2} \tag{12}$$

For example, with the (6,2) forms Eq. (11) can be re-written in the most convenient way

$$a_{-1,i}C_{i-1}^{j'} + a_{0,i}C_i^{j'} + a_{1,i}C_{i+1}^{j'} + a_{2,i}C_{i+2}^{j'} + a_{3,i}C_{i+3}^{j'} + a_{4,i}C_{i+4}^{j'} = b_i^j \tag{13}$$

with

$$\begin{aligned}
a_{-1,i} &= \alpha_{-1} + \frac{fh{\gamma_e}^i}{R_0 + x_i}\beta_{-1}\\
a_{0,i} &= \alpha_0 + \frac{fh{\gamma_e}^i}{R_0 + x_i}\beta_0 - \frac{{\gamma_e}^{2i}}{\lambda}\\
a_{1,i} &= \alpha_1 + \frac{fh{\gamma_e}^i}{R_0 + x_i}\beta_1\\
&\cdots\\
a_{4,i} &= \alpha_4 + \frac{fh{\gamma_e}^i}{R_0 + x_i}\beta_4\\
b_i^j &= -\frac{{\gamma_e}^{2i}}{\lambda}C_i^j
\end{aligned} \tag{14}$$

For each participating species in a given process, an equation equivalent to (13) can be written (exactly the same if all diffusion coefficients are equal and slightly different otherwise [2]) at each node, i, except for $i = 0$. The resulting equations, together with the surface conditions for $i = 0$ and the assumption that $C_i^{j'} = C^{j*} = c^{j*}/c^{r*}$ for $i \geq i_{MAX}$ (with i_{MAX} being the last node of the grid placed at a distance x_{MAX} from the electrode surface), gives rise to a complete system of equations (linear in this case) that can be solved in different ways.

2.2. The Thomas algorithm

With the standard three-point approximation for the space derivatives, the Thomas algorithm has been largely used when semi-infinite conditions hold. Provided that the last point is far enough from the electrode surface for being unaffected by the perturbation at the electrode surface (*i.e.*, $C_{i_{MAX}}^{j'} = C^{j*}$), the backward substitution in the linear system of equations, the combination with the surface conditions and the subsequent forward substitution gives rise to an efficient method to find all the values of $C_i^{j'}$. In the scalar version, this algorithm is only applicable if the profiles of all the participant species are uncoupled. This is to say, they are all independent of each other.

The Thomas algorithm has been extended to asymmetric four-points approximation (4,2) by Britz and Strutwolf [9], by taking a 'post-infinite' point at $i_{MAX} + 1$ where the concentration is also

$C^{j'}_{i_{MAX}+1} = C^{j*}$. This enables a similar two-point backward substitution to be applied. Likewise, for all the (*N*,2) forms, the algorithm can be used by taking $N-3$ 'post-infinite' points and performing a $N-2$ points backward substitution.

2.3. Homogeneous kinetic terms

If homogeneous chemical reactions are present, the profiles of the different species are generally coupled. For example, for the first-order EC mechanism

$$\begin{aligned} &A + e \rightleftarrows B \\ &B \underset{k_{-1}}{\overset{k_1}{\rightleftarrows}} C \end{aligned} \tag{15}$$

the corresponding homogeneous-kinetic terms must be added to Eq. (13). For example, for species *B*, one obtains that

$$a_{-1,i}C^{B'}_{i-1} + a^B_{0,i}C^{B'}_i + a_{1,i}C^{B'}_{i+1} + a_{2,i}C^{B'}_{i+2} + a_{3,i}C^{B'}_{i+3} + a_{4,i}C^{B'}_{i+4} + a^B_{kin}C^{C'}_i = b^B_i \tag{16}$$

where

$$a^B_{0,i} = \alpha_0 + \frac{fh{\gamma_e}^i}{R_0 + x_i}\beta_0 - \frac{{\gamma_e}^{2i}}{\lambda}(1+k_1) \tag{17}$$

$$a^B_{kin} = \frac{{\gamma_e}^{2i}}{\lambda}k_{-1} \tag{18}$$

with k_1 and k_{-1} being the dimensionless rate constants (*i.e.*, the true constants multiplied by the reference time, t_r) for the forward and backward chemical process.

As can be seen, Eq. (16) includes unknown values for the concentration of species *B* and *C*. Therefore, the scalar version of the Thomas algorithm is not applicable but the system of equations remains linear.

2.4. Second-order kinetics

In the case of a system where a second order chemical reaction takes places, for example, a second order EC' (catalytic) mechanism as

$$\begin{aligned} &A + e \rightleftarrows B \\ &B + Z \xrightarrow{k_2} A \end{aligned} \tag{19}$$

the equation corresponding to species *B* in each node is now

$$a_{-1,i}C^{B'}_{i-1} + a_{0,i}C^{B'}_i + a_{1,i}C^{B'}_{i+1} + a_{2,i}C^{B'}_{i+2} + a_{3,i}C^{B'}_{i+3} + a_{4,i}C^{B'}_{i+4} + a^B_{kin2}C^{B'}_i C^{Z'}_i = b^B_i \tag{20}$$

where the last term in the left hand side is non-linear and

$$a^B_{kin2} = \frac{{\gamma_e}^{2i}}{\lambda}k_2 \tag{21}$$

with k_2 being the dimensionless second order rate constant (*i.e.*, the product of the true constant, the reference time t_r and the bulk reference concentration c^{r*}).

3. Numerical calculations

All numerical calculations were carried out in a laptop computer with a Intel® Core i5 processor with 4 Gb of RAM, running under LINUX OpenSuse 13.2, using double precision arithmetic and with the gcc 4.8 compiler. The open source template library for linear algebra Eigen v.3 [10] and the GNU Scientific Library (GSL-1.16), a numerical library for C and C++ programmers [11] were extensively used. All software used is freely available.

4. Results

Digital simulations of electrochemical experiments under a wide range of conditions have been performed making use of the (*N*,2) forms for the finite-difference approximation of the space derivatives and exponentially expanding grids with large values of the expansion factor. Figure 1 shows the dependence of the error of the simulation of a potential step experiment on the expansion factor for several (*N*,2) forms. A fourth-order extrapolation scheme for time integration (EXTRAP4) [5] was employed. Taking, for example, a reference error of 0.1%, the (3,2) form reaches this limit at $\gamma_e \approx 1.1$, whereas the (4,2) form allows for $\gamma_e < 1.67$, the (5,2) form for $\gamma_e < 1$, 8 and with the (6,2) and (7,2) forms γ_e values as high as 1.9 can be attained. Thus, the results obtained with all the above forms (except for the (3,2) one) and very high expansion factors are very satisfactory. However, the highest order forms (7,2) and (8,2) (not shown) tend to oscillate at small values of the expansion factor. Hence, the use of these forms under such conditions is not recommended. Figure 1 corresponds to the case of planar electrodes, although very similar results are obtained for spherical and cylindrical electrodes. For very small electrodes, the upper-limit values of γ_e are a bit smaller, in the range 1.5–1.8 for the forms (4,2) to (7,2).

The use of very high expansion factors allows for accurate simulation with very few discrete points in the concentration profiles. This is shown in Figure 2 for a potential step at a spherical electrode with $R_0 = 1$. In a real experiment with a step duration of 1 s and a diffusion coefficient of 6.25×10^{-6} cm^2 s^{-1}, the above R_0-value corresponds to a spherical electrode of $r_0 = 25$ μm. As can be seen, the error remains around 0.1% for 95% of the experiment with only 8 points in the concentration profile. The error slightly improves with 9-points and it is very similar for higher number of points.

As stated above, the (*N*,2) forms are suitable for being used with the Thomas algorithm, which is well known for its good performance in speed. However, given the very few points required for the simulations with these high-order forms, it is reasonable to consider the 'brute force' resolution of the corresponding system of equations. To do this, three different approaches have been tested

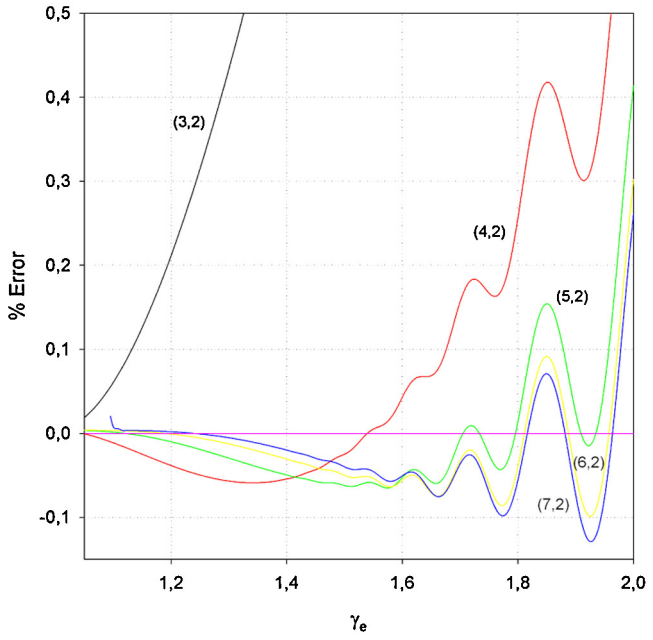

Figure 1. Dependence of the error (%) on the expansion factor, γ_e, in the simulation of a limiting current potential step at a planar electrode for different (*N*,2) forms (indicated on the curves). EXTRAP4, $\delta\tau = 0.01$, $\tau = 1$, $h = 0.05$, $x_{MAX} = 6$.

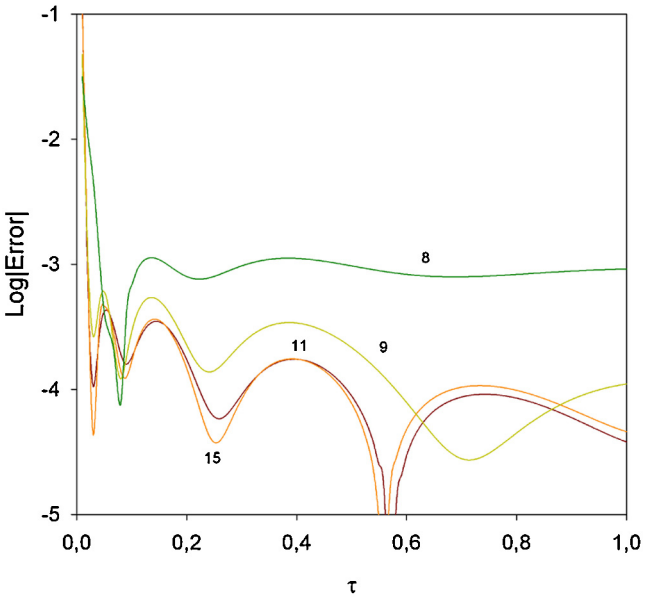

Figure 2. Log|Error| in the simulation of a limiting current potential step at a spherical electrode using the (6,2) form and different numbers of points in the spatial grid (indicated on the curves). EXTRAP4, $\gamma_e = 1.67$, $\delta\tau = 0.01$, $x_{MAX} = 6$, $R_0 = 1$.

in this work for the case of linear (or linearized) problems. First, the standard dense-matrix techniques, LU and QR decompositions, have been employed, both of them by following the routines provided by the GSL (Gnu Scientific Library) [11]. Also, techniques for sparse matrices have been assessed. For this purpose, the sparse module of EIGEN [10], EIGEN_SP, has been employed. The best performing technique depends on the problem considered. In Figure 3 the relative performance of the different algorithms is plotted *versus* the number of unknowns (*i.e.*, the concentration of all species in all grid points). For example, with 15 points *per* profile and the EC mechanism (which involves 3 species), the total number of unknowns is 45. As can be expected, the routines for dense matrix computations work very well for relatively dense matrices. Conversely, the use of EIGEN_SP is more competitive as the matrix sparsity increases.

The above behaviour is illustrated in Figure 3. Thus, Figure 3a refers to a potential step experiment with a second order extrapolation (EXTRAP2) scheme for time integration [5]. Under these conditions, only three matrix inversions are needed to simulate the complete experiment (the matrix of coefficients remains unchanged but there are three different matrices due to the interval subdivision of the EXTRAP2 method). As can be seen, the matrix-dense algorithms are faster than the Thomas algorithm while the number of unknowns is lower than 60 (this covers all practical situations for one-dimensional semi-infinite problems). Regarding the sparse-matrix algorithm, this is always faster than Thomas, the performance gain increasing with the number of unknowns.

The situation is different when the surface conditions are time-dependent. This occurs, for example, when a potential-scan is applied. With standard LU decomposition, a *complete* matrix factorization is required at each time step, which strongly compromises its performance. However, when only one row of the matrix changes (which is the case of the simulation of a potential scan), the QR decomposition enables a rank-1 update of the factorized matrix making unnecessary the complete factorization process. Hence, QR is clearly advantageous (and competitive against Thomas) compared with LU. With respect to the sparse matrix routine EIGEN_SP, there are two different steps in a complete decomposition. In the first one, the structure of the matrix is analysed searching for the columns permutations that give rise to the maximum sparsity of the factorised LU matrix. In the second step, the numerical factorization is performed. Given that the sparsity pattern of the matrix is always the same in the problems considered here, the *a priori* matrix analysis is executed only once (whereas the numerical factorization is made at each time step). As a consequence, the performance of EIGEN_SP is very comparable with Thomas' in all conditions as shown in Figure 3b, with a slight improvement of EIGEN_SP as the number of unknowns (and the sparsity of the matrix) increases.

It is important to bear in mind that the Thomas algorithm is only applicable when the concentration profiles of the different species

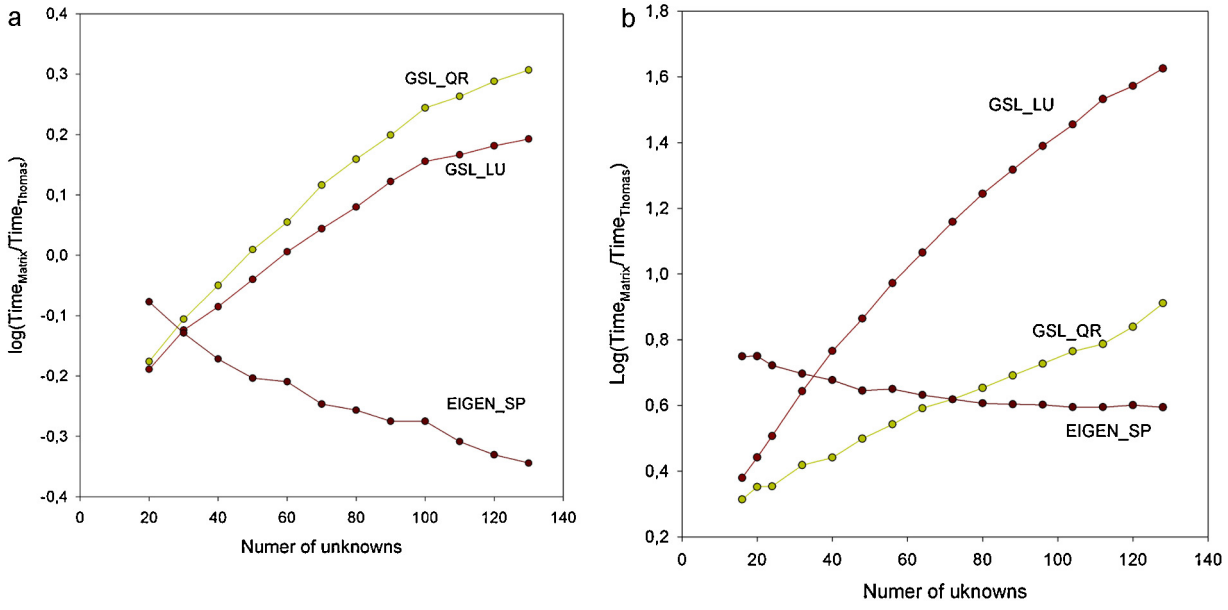

Figure 3. (a) Cpu-time of the three matrix algorithms considered ($Time_{Matrix}$) with respect to the Thomas algorithm ($Time_{Thomas}$) as a function of the number of unknowns in the simulation of a potential step experiment. EXTRAP2, $\delta\tau = 0.001$, (5,2) form, simple charge transfer reaction. (b) Cpu-time of the three matrix algorithms considered ($Time_{Matrix}$) with respect to the Thomas algorithm ($Time_{Thomas}$) as a function of the number of unknowns in the simulation of a 1000-point potential scan. FI, (5,2) form, simple charge transfer reaction.

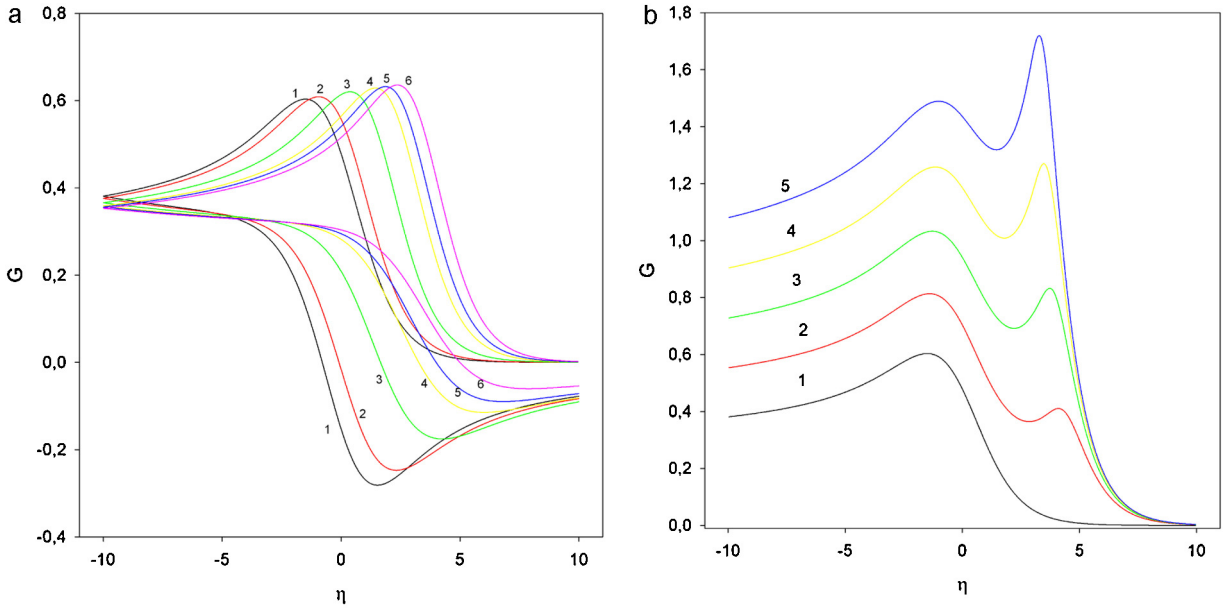

Figure 4. (a) Cyclic voltammograms of a first-order EC mechanism (15) obtained using the (6,2) form with a 14-point grid ($h = 0.051$, $\gamma_e = 1.67$) and QR decomposition for different values of the dimensionless rate constant k_1: 0(1), 10(2), 100(3), 500(4), 1000(5) and 2500(6). $k_{-1} = 10$ FI integration, $\delta\tau = 0.025$, $R_0 = 5$, $x_{MAX} = 60$. (b) Linear sweep voltammograms of a second order EC' mechanism (19) obtained using the (6,2) form with a 14-point grid ($h = 0.051$, $\gamma_e = 1.67$) and the EIGEN_SP routine for different values of C^{Z*}: 0(1), 0.5(2), 1(3), 2(4) and 3(5). FI integration, $k_2 = 10\,000$, $\delta\tau = 0.025$, $R_0 = 5$. $\eta = \frac{nF}{RT}(E - E^0)$, $G = I(RT)^{1/2}/F^{3/2}qD_A^{1/2}C_A^*\nu^{1/2}$ and $t_r = RT/F\nu$ where ν is the scan rate, q the electrode area, I the current and other symbols have their usual meaning.

are not coupled. Hence, when homogeneous chemical reactions are present, direct matrix decomposition is the most suitable choice either in the sparse- or dense-matrix alternatives. If only first-order chemical reactions are present, the selection of the most appropriate decomposition method can be made following the above discussion. For example, in Figure 4a the cyclic voltammograms obtained for the EC mechanism (15) with a 14-point grid and the (6,2) form are shown for a spherical electrode with $R_0 = 5$ and several values of the dimensionless rate constant k_1.

Attending to the numbers of unknowns (42) and the results shown in Figure 3b, the QR decomposition was employed in the simulations. The runtime of each voltammogram was always shorter than 15 ms in a modest laptop computer with an Intel Core i5 processor. It is worth pointing out that the curves obtained with the 14-point grid superimpose exactly with those obtained with a much more refined grid with $\gamma_e = 1.02$ and 200 points.

As stated above, when a second order chemical reaction is present, the system of equations is non linear. A first attempt to solve this system is to develop a linear approximation as suggested in [2]. For the kinetic term in the second order EC' mechanism (19), the following approximation is taken for the last term in the left hand side of (20)

$$a^B_{kin2} C_i^{B'} C_i^{Z'} \approx a^B_{kin2}(C_i^{B'} C_i^Z + C_i^B C_i^{Z'} - C_i^B C_i^Z) \tag{22}$$

With this approximation, some coefficients in all rows of the matrix are different in each time step as a consequence of the inclusion of the 'old' concentration values (C_i^B and C_i^Z in (22)). Hence, there are no benefits in using the QR method. On the other hand, EIGEN_SP is particularly advantageous since the sparsity pattern remains unchanged.

Initially, the values of the concentrations obtained with the linear approximation (22) were to be used as initial guess for Newton's method. However, the concentrations obtained with the linearization approach were so close to the true values that the approximation can be considered acceptable.

In Figure 4b, several linear sweep voltammograms obtained for the second order EC' mechanism are shown. As in Figure 4a, the curves were obtained with a 14-point grid and the (6,2) form, finding a complete superposition with the results obtained with a 200-point grid and spending about 30 ms of real computation time *per* voltammogram.

The computer programs needed to develop the 'brute force' approach presented here are very simple, but they can be a bit tedious in two specific points: the calculation of the coefficients α and β, and the filling of the matrix. For these reasons, a small set of (fully functional) example programs are provided. This includes a tested routine to calculate α and β for a complete set of situations and routines to fill in the matrices taking into account that, by the nature of the proposed method, no special care is needed in the order of filling or in the position of non-zero values. These examples (source and header C++ files) can be found in Supplementary Material.

5. Conclusions

With the use of asymmetric (N,2) forms to approximate the spatial derivatives in finite-difference methods for digital simulation of electrochemical problems, the concentration profiles can be accurately described with grids containing less than 15 points. Under these conditions, the direct ('brute force') resolution of the finite difference equation system has been proven to be very competitive in a wide range of situations. Direct LU decomposition is recommended for time-independent surface conditions and no changes in the matrix of coefficients (for example, potential step experiments with no homogeneous chemical reactions or with only first order chemical reactions), QR decomposition is advantageous when small changes in the matrix of coefficients occur (for example, potential scan experiments in systems with only first-order homogeneous chemical reactions) and sparse matrix routines, such as EIGEN_SP, are particularly valuable when the values in the coefficient matrix change strongly at each time step (as, for example, when second order chemical reactions take place) or when the total number of unknowns 'number of species × number of grid nodes' is very high

(for example, reaction mechanisms with quite a few participating species).

All the needed computer programs are very simple and totally accessible to the occasional programmer. Moreover, routines for the more tedious steps and fully operative real example programs are provided. All the routines and programs needed are freely available on Internet.

Acknowledgments

The authors greatly appreciate the financial support provided by the Ministerio de Economia y Competitividad (Project Number CTQ2012-36700, co-funded by European Regional Development Fund) and by the Fundación Séneca de la Región de Murcia under the III PCTRM 2011-2014 Programme (Projects 18968/JLI/13, 19456/PI/14 and 19320/PI/14).

Appendix A. Supplementary data

Supplementary data associated with this article can be found, in the online version, at doi:10.1016/j.cplett.2015.11.011.

References

[1] D. Britz, J. Electroanal. Chem. 406 (1996) 15.
[2] D. Britz, Digital Simulation in Electrochemistry, Springer, 2005.
[3] L. Thomas, Comput. Lab. Rept., Columbia University, 1949.
[4] M. Rudolph, J. Electroanal. Chem. 314 (1991) 13.
[5] J. Strutwolf, D. Britz, Comput. Chem. 25 (2001) 511.
[6] D. Britz, Electrochem. Commun. 5 (2003) 195.
[7] F. Martínez-Ortiz, N. Zoroa, Á. Molina, C. Serna, E. Laborda, Electrochim. Acta 54 (2009) 1042.
[8] F. Martínez-Ortiz, A. Molina, E. Laborda, Electrochim. Acta 56 (2011) 5707.
[9] D. Britz, J. Strutwolf, Comput. Biol. Chem. 27 (2003) 327.
[10] G. Guennebaud, B. Jacob, et al., Eigen v3, 2010, http://eigen.tuxfamily.org.
[11] J.D.M. Galassi, J. Theiler, B. Gough, G. Jungman, P. Alken, M. Booth, F. Rossi, GNU Scientific Library Reference Manual, third edn., Network Theory Ltd., 2009.